Trapping effects in a self-gravitating quantum dusty plasma

2011 Phys. Scr. 84 045505

(http://iopscience.iop.org/1402-4896/84/4/045505)

Phys. Scr. **84** (2011) 045505 (8pp) doi:10.1088/0031-8949/84/04/045505

Trapping effects in a self-gravitating quantum dusty plasma

M Ayub[1,2], H A Shah[1] and M N S Qureshi[1]

[1] Department of Physics, GC University, Lahore 54000, Pakistan
[2] Department of Physics, Government Science College, Panjeri A K, Pakistan

E-mail: nouman_sarwar@yahoo.com

Received 13 July 2011
Accepted for publication 5 September 2011
Published 3 October 2011
Online at stacks.iop.org/PhysScr/84/045505

Abstract
The effects of trapping on the nonlinear properties of dust-acoustic waves in an unmagnitized collisionless self-gravitating plasma were studied by treating the ions to be Maxwellian, the dust to be cold and the electrons to be degenerate. The effect of trapping and the gravitational potential on the nonlinear structures was investigated by employing the Sagdeev potential approach, which shows that the features of solitary wave structures are affected by changes in Mach number as well as ion temperature and other physical parameters of the system. Modulational stability analysis is also presented, and the regions of stability and instability are discussed.

PACS numbers: 52.27.Lw, 52.35.Mw, 52.35.Sb

1. Introduction

Over the last decade, interest in the study of degenerate plasmas has increased considerably, unanimously accepting the importance of the quantum nature of electrons in highly dense plasmas or extremely cold plasmas [1–7]. In both situations, the thermal wavelength $\lambda_B = (2\pi^2\hbar^2/m_a k_B T)^{1/2}$ is of the same order as the interparticle distance ($d = n^{-1/3}$) or the Fermi–Debye length λ_{DF} ($= (\lambda_{DFe}^2\lambda_{Di}^2/\lambda_{DFe}^2 + \lambda_{Di}^2)^{1/2}$) and consequently $n_a\lambda_B^3 \approx 1$, then we have an overlap of the probability clouds. In these circumstances, plasma particles are supposed to be indistinguishable. The quantum mechanical interaction appears among the neighboring particles due to which the collective behaviour changes. Over the last few years, quantum study of plasma has gained impetus because of its versatile applications in microelectronics [8], laser-produced plasma and dense astrophysical objects [9–11]. In these papers, quantum statistical effects have been incorporated by including the Fermi pressure term, and the quantum diffraction or scattering effects are governed by a double differential term called the Bohm potential term in the fluid model [12–15]. The fluid model has been used for both linear [16–17] and nonlinear analyses of different wave modes [18–21]. Many theoretical researchers have developed the Korteveg–de Vries (KdV) equation, the modified KdV equation, the nonlinear Schrödinger equation and the Burgers equation [1–3, 20–22] to study the nonlinearities in degenerate quantum plasmas. Recently [23], the Sagdeev potential approach was used to investigate solitary wave solutions in electron–ion quantum plasma.

Dusty degenerate plasmas can be found both in astrophysical bodies and in the laboratory. It is now evident that dust clouds can be present around white dwarfs [24], which can contaminate their surfaces. Dust may also be added to white dwarfs when a star swells into a red giant and the planets moving around it are engulfed by it. These objects are turned into dust grains due to the frictional forces and, after the supernova phase, a white dwarf may appear with dust grains. In microelectro-mechanical systems, ultra-small electronic devices and laser-produced plasmas, impurities play the role of dust particles [25–27]. Thus, once dust is present, it plays an important role in the modification of plasma species dynamics. In the examples given above, densities are high enough to make the plasma degenerate. We point out here that in most situations, only electrons are considered to be quantum or degenerate owing to their small mass, and heavier particles such as ions or charged dust are treated classically.

Many papers have been published in relation to the inclusion of quantum effects in the study of dusty plasmas, e.g. Shukla and Ali [28] studied the modification of dust-acoustic waves in unmagnetized dusty quantum plasma. Salimullah *et al* [29] discussed quantum effects using the

quantum hydrodynamic model on the linear dispersion relation of dust lower-hybrid waves. Quantum effects cannot be ignored in dense astrophysical environments such as white dwarfs and neutron stars. In such systems the thermal pressure is balanced by the inward gravitation force. Therefore, we cannot ignore the effects of gravity which are included via the Jean term. Many authors have addressed the Jean instability in quantum plasmas [5, 30–33].

Nonlinear dynamics is affected by the trapping of particles. It has been verified that the trapping, as considered by us, is a microscopic phenomenon through computer simulations [34] and experimental investigations [35]. Gurevich [36] showed, using Vlasov's equation along with Maxwell's equations, that the adiabatic trapping produces 3/2 power nonlinearity (for Maxwellian plasma) rather than the usual quadratic type of nonlinearity in the absence of trapping. In classical plasmas, the effects of trapping on the nonlinear characteristics of plasma waves and on vortex formation are well investigated [37]. To date, only a small amount of work has been done on trapping effects in quantum plasmas. Luque *et al* [38] considered first time quantum trapping corrections by solving the Wigner–Poisson system in an electron–hole plasma. The effect of trapping in degenerate plasmas was recently investigated [39], where the Fermi–Dirac distribution function was used to determine the number density of free and trapped particles. The effect of trapped particles led to a new type of nonlinearity, and further investigation showed that under certain conditions it is possible to obtain both compressive and rarefactive solitary structures. Misra and Chowdhury [40] studied dust-acoustic waves in a self-gravitating complex plasma with trapped electrons and also performed linear stability analysis. As dust grains are strongly expected to be present in extremely dense plasmas, so trapping with quantum effects on nonlinear structures becomes important in the investigation of self-gravitating plasmas in dense astrophysical plasmas. To the best of our knowledge, trapping with both quantum and gravitational effects has not yet been studied.

In this paper, we study the dust-acoustic waves in a self-gravitating dusty plasma with trapping of electrons that are taken to be degenerate. In section 2, mathematical formulation is presented and the linear dispersion relation is derived for dust-acoustic waves taking into account the quantum effects. In section 3, electrostatic and gravitational Sagdeev potentials are developed to study the nonlinear behaviour of these waves. The solitary waves and respective soliton structures are discussed in section 4. Modulational stability analysis is discussed in section 5, and our conclusions are presented in the final section.

2. Mathematical formulation

We consider a three-component plasma consisting of degenerate electrons, classical ions and negatively charged dust grains that, due to their mass, are treated as cold. In the presence of charged dust particles, both electrons and ions are taken to be massless. The fluid equation of motion for dust grains can be written as

$$m_{\mathrm{d}}n_{\mathrm{d}}\left\{\frac{\partial\vec{v}_{\mathrm{d}}}{\partial t}+(\vec{v}_{\mathrm{d}}\cdot\vec{\nabla})\vec{v}_{\mathrm{d}}\right\}=Z_{\mathrm{d}}en_{\mathrm{d}}\vec{\nabla}\varphi-m_{\mathrm{d}}n_{\mathrm{d}}\vec{\nabla}\phi, \quad (1)$$

and the equation of continuity is as usual given by

$$\frac{\partial\vec{v}_{\mathrm{d}}}{\partial t}+\vec{\nabla}\cdot n_{\mathrm{d}}\vec{v}_{\mathrm{d}}=0, \quad (2)$$

where m_{d}, n_{d}, Z_{d} and φ and ϕ are the dust mass, dust number density, dust charge number and electrostatic and gravitational potentials, respectively.

The electrostatic and gravitational Poisson equations are, respectively,

$$\nabla^2\varphi=4\pi\, e(Z_{\mathrm{d}}n_{\mathrm{d}}+n_{\mathrm{e}}-n_{\mathrm{i}}), \quad (3)$$

$$\nabla^2\phi=4\pi\, Gm_{\mathrm{d}}n_{\mathrm{d}}. \quad (4)$$

Here, n_{i} and n_{e} are the number densities of the ions and electrons, respectively, and G is the gravitational constant. We can incorporate the dust charge fluctuations as has been done in many previous classical works [41], but this will not change the behaviour of the system qualitatively and will only cause unnecessary mathematical detail. If the dust dynamics is slower than the dust charging time, then we can safely ignore the dust charge fluctuations. We would also like to point out that it has been shown by Tsintsadze and Tsintsadze [42] that a dust grain may only be taken as a point particle with constant charge, as is dictated by the available electrodynamics theory. We consider one-dimensional (1D) perturbations in the x-direction only and shift to a comoving frame of reference with velocity u; by defining a new variable $\zeta=x-ut$, this then makes it possible to integrate equations (1) and (2) and thus we obtain

$$n_{\mathrm{d}}=n_{\mathrm{d0}}\left\{1+\frac{2}{u^2}\left(\frac{Z_{\mathrm{d}}\,e\varphi}{m_{\mathrm{d}}}-\phi\right)\right\}^{-1/2}. \quad (5)$$

We have employed 'Jean's swindle' here (ignoring the zeroth-order gravitational field) [43] and have used the following boundary conditions: when $\zeta\to\infty$, all perturbations vanish, i.e. v_{d}, φ, $\phi\to 0$ and $n_{\mathrm{d}}\to n_{\mathrm{d0}}$. We further note that for n_{d} to be real, the condition

$$\phi\leqslant\frac{u^2}{2}+\frac{Z_{\mathrm{d}}e\varphi}{m_{\mathrm{d}}}$$

must be fulfilled.

In order to compute the number density of the degenerate electrons, we use the Fermi–Dirac distribution [44] and, through integration with respect to energy ε, we obtain an expression for the number density of electrons,

$$n_{\mathrm{e}}(\varepsilon)=\frac{8\sqrt{2}\pi m_{\mathrm{e}}^{3/2}}{(2\pi\hbar)^3}\int_0^\infty\frac{\varepsilon^{1/2}}{\exp\left[\varepsilon-(\mu/T_{\mathrm{e}})\right]+1}\,\mathrm{d}\varepsilon,$$

where μ is the chemical potential. However, in the case when the electrons are trapped due to an electrostatic potential φ, we follow the work of Shah *et al* [39] to obtain

$$n_{\mathrm{e}}(r,t)=\frac{8\sqrt{2}\pi\, m_{\mathrm{e}}^{3/2}}{(2\pi\,\hbar)^3}\left[\frac{2}{3}U^{3/2}+\frac{\pi^2T_{\mathrm{e}}^2}{12}U^{-1/2}\right], \quad (6)$$

where temperature T_{e} is considered to be small and higher-order terms in T_{e} are neglected, and we substitute $U=e\varphi+\mu$.

For a completely degenerate plasma, $T_e = 0$, and the chemical potential is

$$\mu = \varepsilon_F = \frac{\hbar^2}{2m_e}(3\pi^2 n_{e0})^{2/3},$$

where ε_F is the Fermi energy. In the fully degenerate case, equation (6) reduces to

$$n_e = n_{e0}\left(1 + \frac{e\varphi}{\varepsilon_F}\right)^{3/2}. \tag{7}$$

The ions are considered as classical particles since their mass is much larger than that of electrons; however, on the other hand, the ion mass is much smaller than the dust mass; thus it is reasonable to assume that the ions follow the Boltzmann distribution, which is given by

$$n_i = n_{i0}\, e^{-e\varphi/T_i}, \tag{8}$$

where n_{i0} and T_i are, respectively, the equilibrium ion number density and ion temperature.

Linearizing equations (1)–(5), (7) and (8) gives the linear dispersion relation of dust-acoustic waves in quantum dusty plasma in which fermionic electrons assist the thermal ions in propagating the wave. The linear dispersion relation takes the form

$$\omega^2 + \omega_{jd}^2 = \frac{c_{sF}^2 k^2}{1 + k^2\lambda_{DF}^2}. \tag{9}$$

Here, $\omega_{jd} = \sqrt{4\pi\, G\, m_d n_{d0}}$ is the Jean frequency; $c_{sF} = \omega_{pd}\lambda_{DF}$ is the speed of sound; $\omega_{pd} = \sqrt{\frac{4\pi\, n_{d0} Z_d^2 e^2}{m_d}}$ is the dust plasma frequency; and λ_{DF} is the Debye length with quantum effects, which can be written as

$$\frac{1}{\lambda_{DF}^2} = \frac{1}{\lambda_{DFe}^2} + \frac{1}{\lambda_{Di}^2},$$

where

$$\lambda_{DFe}^2 = \frac{\varepsilon_F}{6\pi n_{e0} e^2} \quad \text{and} \quad \lambda_{Di}^2 = \frac{T_i}{4\pi n_{i0}\, e^2}.$$

In the long wavelength limit, $k^2\lambda_{DF}^2 \ll 1$, the dispersion relation simplifies to

$$\omega^2 + \omega_{jd}^2 = c_{sF}^2 k^2. \tag{10}$$

If we suppose that the electrons predominantly define the Debye length, then the speed of sound is

$$c_{sF}^2 = \frac{2\varepsilon_F}{3m_d}\left(\frac{n_{d0} Z_d^2}{n_{e0}}\right).$$

From equation (10), using some typical quantum dusty plasma parameters such as [45, 46] $m_d = 10^{-12}$ g, $n_{e0} = 10^{26}$ cm^3 and $n_{d0} = 10^{19}$ cm^3, we obtain the condition for the real solution of the dust-acoustic frequency ω, i.e. $\lambda(= 2\pi/k) < 13.6$ cm; the thermal length (de Broglie length) is evaluated to be 4.5×10^{-9} cm, which is longer than the Fermi–Debye length (λ_{DF}) in our system that turns out to be 2.88×10^{-9} cm. Observations [47] made with the Spitzer Space Telescope for a white dwarf show that most of the dust grains have a diameter less than 0.2 μm. As we are mainly considering the dusty plasma surrounding a white dwarf, we have a wide range of wavelengths for dust-acoustic waves (DAWs) in which the quantum effects can be considered and the size of the dust grains can be neglected, making it possible to treat the charged dust particles as point particles.

3. Nonlinear treatment

In this section, we investigate solitary wave structures by using the Sagdeev potential approach. Using equations (5), (7) and (8) in equation (3), and equation (5) in equation (4), and following the procedure developed in [39], we obtain, respectively, for the electrostatic and gravitational potentials

$$\frac{d^2\varphi}{d\zeta^2} = 4\pi e\left[Z_d n_{d0}\left\{1 + \frac{2}{u^2}\left(\frac{Z_d e\varphi}{m_d} - \phi\right)\right\}^{-1/2} + n_{e0}\left(1 + \frac{e\varphi}{\varepsilon_F}\right)^{3/2} - n_{i0}\, e^{-e\varphi/T_i}\right], \tag{11}$$

$$\frac{d^2\phi}{d\zeta^2} = 4\pi\, G m_d n_{d0}\left\{1 + \frac{2}{u^2}\left(\frac{Z_d\, e\varphi}{m_d} - \phi\right)\right\}^{-1/2}. \tag{12}$$

After some algebraic manipulation, equations (11) and (12) can be rewritten, respectively, as

$$\frac{1}{2}\left(\frac{d\varphi}{d\zeta}\right)^2 + V_E(\varphi, \phi) = 0, \tag{13}$$

$$\frac{1}{2}\left(\frac{d\phi}{d\zeta}\right)^2 + V_G(\varphi, \phi) = 0. \tag{14}$$

Here, equations (13) and (14) are analogous to the energy integral of a classical particle in a 1D potential well and $V_E(\varphi)$ and $V_G(\phi)$ are the electrostatic and gravitational Sagdeev potentials, respectively, which are given by

$$V_E = 4\pi\, n_{i0}\varepsilon_F \times\left[\frac{2\,\gamma_1^2 Z_d^2 M^2}{3\gamma_2}\left\{1 - \left(1 + \frac{3\gamma_2}{\gamma_1 Z_d^2 M^2}\,(Z_d\Phi - \Psi)\right)^{1/2}\right\} + \frac{2}{5}\gamma_2\left\{1 - (1+\Phi)^{5/2}\right\} + T_i\left(1 - e^{-\Phi/T_i}\right)\right], \tag{15}$$

$$V_G = \frac{8\pi\, G\, n_{d0}\varepsilon_F\gamma_1 Z_d^2 M^2}{3\gamma_2}\left[\left\{1 + \frac{3\gamma_2}{\gamma_1 Z_d^2 M^2}\,(Z_d\Phi - \Psi)\right\}^{1/2} - 1\right], \tag{16}$$

where $\gamma_1 = \frac{n_{d0}}{n_{i0}}$ and $\gamma_2 = \frac{n_{e0}}{n_{i0}}$ are the normalized dust and electron number densities, respectively; $M = \frac{u}{c_{sF}}$ is the Mach number; $\Phi = \frac{e\varphi}{\varepsilon_F}$ and $\Psi = \frac{m_d\phi}{\varepsilon_F}$ are, respectively, the normalized electrostatic and gravitational potential energies; and $T_i = \frac{T_i}{\varepsilon_F}$ is the normalized ion temperature.

4. Solitary waves in the absence of the Jean term

In this section, we consider the formation of solitary structures when the Jean term is absent. In this case the electrostatic Sagdeev potential given by equation (15) reduces to

$$V(\Phi) = 4\pi\, n_{i0}\varepsilon_F\left[\frac{2\,\gamma_1^2 Z_d^2 M^2}{3\gamma_2}\left\{1 - \left(1 + \frac{3\gamma_2}{\gamma_1 Z_d M^2}\Phi\right)^{1/2}\right\} + \frac{2}{5}\gamma_2\left\{1 - (1+\Phi)^{5/2}\right\} + T_i\left(1 - e^{-\Phi/T_i}\right)\right]. \tag{17}$$

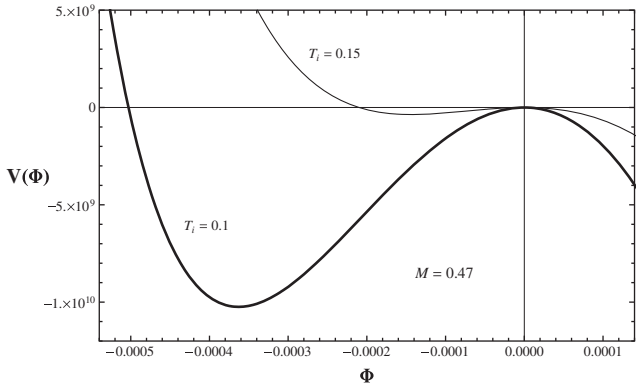

Figure 1. Profile of the Sagdeev potential $V(\Phi)$ for different values of $T_{\rm i}$, the other parameters being $M = 0.47$, $\gamma_1 = 10^{-5}$ and $n_{\rm i0} = 10^{26}\,{\rm cm}^{-3}$.

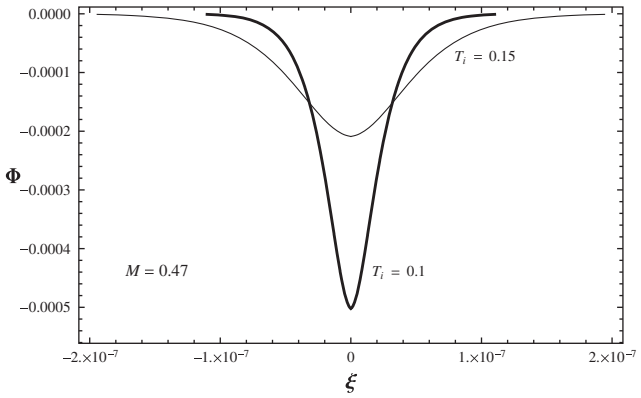

Figure 2. Soliton structures for different values of $T_{\rm i}$ corresponding to $V(\Phi)$ in figure 1.

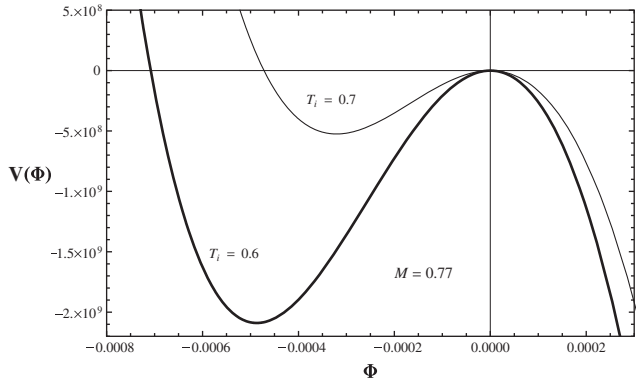

Figure 3. Profile of $V(\Phi)$ for different values of $T_{\rm i}$, the other parameters being $M = 0.77$, $\gamma_1 = 10^{-5}$ and $n_{\rm i0} = 10^{26}\,{\rm cm}^{-3}$.

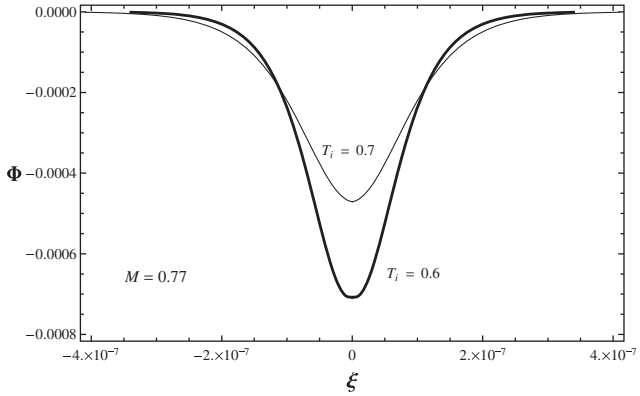

Figure 4. Soliton structures for different values of $T_{\rm i}$ corresponding to $V(\Phi)$ in figure 3.

From equation (17), the nonlinear solution can be obtained if $V(\Phi) < 0$. Following Witt and Lotko [48], we see that a solitary wave solution is possible when the Mach number $M > Z_{\rm d}\sqrt{\gamma_1 T_i/2 + 3\gamma_2 T}$; the Sagdeev potential satisfies the conditions $\frac{{\rm d}V(\Phi)}{{\rm d}\Phi} = 0$ and $\frac{{\rm d}^2V(\Phi)}{{\rm d}\Phi^2} < 0$ at $\Phi = 0$ and $\frac{{\rm d}V(\Phi)}{{\rm d}\Phi} < 0$ at $\Phi = -\Phi_0$ and $-\Phi_0 < \Phi < 0$, where $-\Phi_0$ is the minimum value of the electrostatic potential. Hence, equation (17) admits a corresponding solitary wave solution. The solitary wave solution of equation (16) cannot be obtained, as the above-mentioned conditions are not satisfied for the case of a gravitational Sagdeev potential. Thus in this section we have taken into account only the electrostatic potential.

In figures 1–8, we numerically analyze the electrostatic potential (equation (17)) considering the electron trapping with quantum effects. In the numerical calculations, we have taken the plasma species number density to be fixed and investigated the effects on the Sagdeev potential and the corresponding soliton structures by varying the ion temperature and Mach number. Figure 1 depicts the profiles of the electrostatic Sagdeev potential for different values of $T_{\rm i}$ when the Mach number is fixed at $M = 0.47$. Rarefactive soliton structures corresponding to the Sagdeev potentials given in figure 1 are shown in figure 2 for the same plasma parameters. We see that for smaller values of $T_{\rm i}$ the soliton amplitude increases and the width decreases. We plot figure 3 for higher values of M and $T_{\rm i}$ as compared with figure 1. Figures 3 shows the profiles of the Sagdeev potential for different values of $T_{\rm i}$ at the fixed value of Mach number $M = 0.77$. Rarefactive soliton structures corresponding to the Sagdeev potentials given in figure 3 are shown in figure 4 for the same plasma parameters. We can see that the variation in $T_{\rm i}$ affects the soliton amplitude less strongly at larger values of Mach number as compared to figure 2. At smaller value of $T_{\rm i}$, the soliton amplitude increases and the width decreases as compared to larger values. Moreover, a comparison of figures 2 and 4 shows that the soliton amplitude increases with increasing Mach number.

Sagdeev potential profiles for different values of Mach number M=0.44 and 0.5 and the fixed value of $T_{\rm i} =$ 0.1 are shown in figure 5. Rarefactive soliton structures corresponding to the Sagdeev potentials given in figure 5 are shown in figure 6 for the same plasma parameters. We note that with an increase in Mach number M, the soliton amplitude increases and the width decreases when $T_{\rm i}$ is kept constant. The profiles of the Sagdeev potential for the soliton structure for higher values of Mach number in the subsonic regime at a fixed value of $T_{\rm i}$ are shown in figure 7. Rarefactive soliton structures corresponding to the Sagdeev potentials given in figure 7 are shown in figure 8 for the same plasma parameters. Again we can note that the variation in Mach number M affects the soliton structure when $T_{\rm i}$ is kept constant. But the increase in soliton amplitude is more sensitive to the value of M when $T_{\rm i}$ is set at higher value. On the other hand, comparing figures 6 and 8 we note that the soliton amplitude increases for smaller values of $T_{\rm i}$ in the subsonic regime.

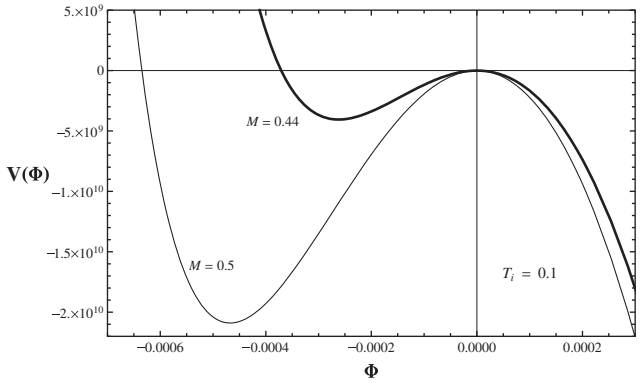

Figure 5. Profile of $V(\Phi)$ for different values of Mach number M, the other parameters being $T_{\rm i} = 0.1$, $\gamma_1 = 10^{-5}$ and $n_{\rm i0} = 10^{26}\,{\rm cm}^{-3}$.

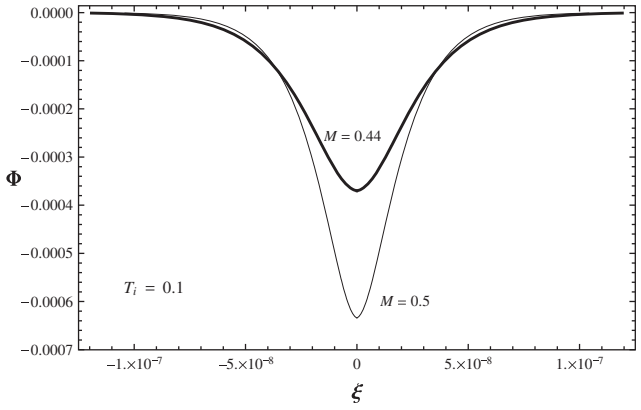

Figure 6. Soliton structures for different values of M corresponding to $V(\Phi)$ in figure 5.

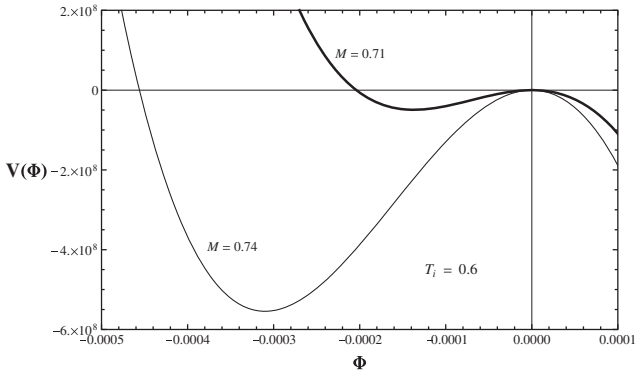

Figure 7. Profile of $V(\Phi)$ for different values of M when the other parameters are $T_{\rm i} = 0.6$, $\gamma_1 = 10^{-5}$ and $n_{\rm i0} = 10^{26}\,{\rm cm}^{-3}$.

Further, we investigate the effects of changes in dust charge number, ion number density and the ratio of the dust number density to the ion number density on the Sagdeev potential and the structure of the solitons. These are the parameters that specify the quantum behavior of the system. Figure 9 presents the behavior of the Sagdeev potential for different values of the dust charge number $Z_{\rm d}$ and the corresponding soliton structures are presented in figure 12. We note that the amplitude of the soliton increases with a decrease in $Z_{\rm d}$, whereas the width shows the opposite behavior. Soliton structures of the solitary waves shown in figure 10 are depicted in figure 13, which shows that the amplitude is not affected by changes in $n_{\rm i0}$ provided that γ_1 is kept constant. On the other hand, the width of the soliton increases with a decrease in ion number density. The Sagdeev potential profile in figure 11 shows that the solitary wave structures are strongly affected by changes in the ratio γ_1. The corresponding change in the amplitude of solitons is shown in figure 14. It is clear that the amplitude increases with a decrease in the value of γ_1, which is evidence again that the dust density effectively changes the soliton structure. We note that in obtaining the above graphical analysis the quasi-neutrality condition was consistently taken into account.

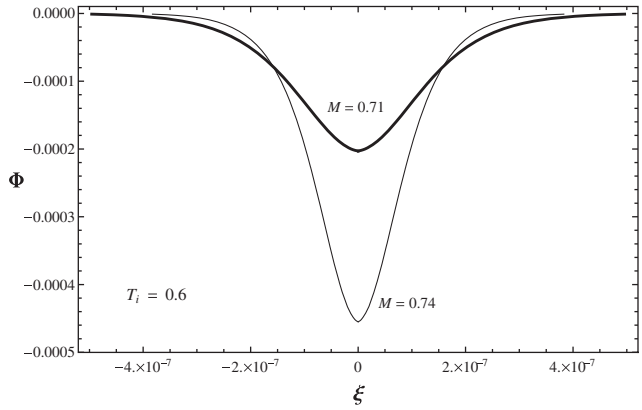

Figure 8. Soliton structures for different values of M corresponding to $V(\Phi)$ in figure 7.

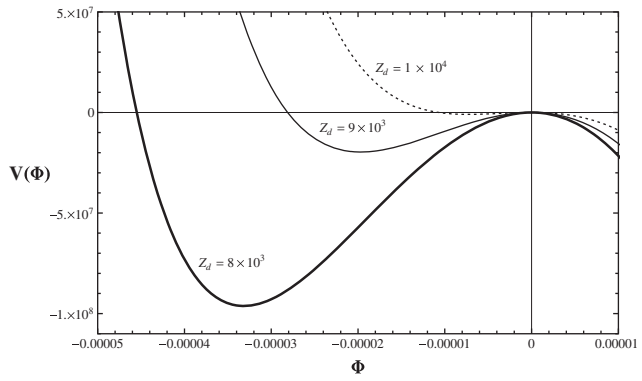

Figure 9. Profile of $V(\Phi)$ for different values of dust charge number $Z_{\rm d}$ when the other parameters are $M = 0.38$, $T_{\rm i} = 0.1$, $\gamma_1 = 10^{-7}$ and $n_{\rm i0} = 10^{26}\,{\rm cm}^{-3}$.

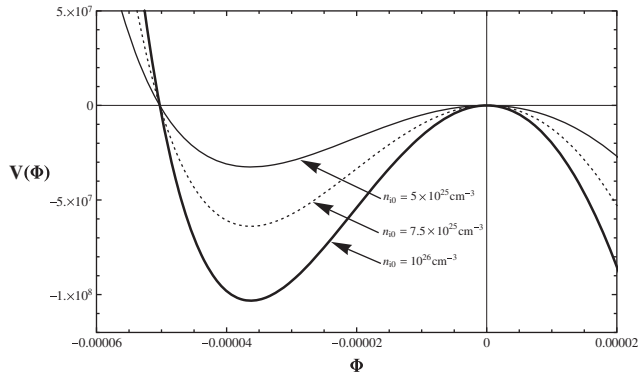

Figure 10. Profile of $V(\Phi)$ for different values of $n_{\rm i0}$ when the other parameters are $M = 0.47$, $T_{\rm i} = 0.1$, $Z_{\rm d} = 10^4$, $\gamma_1 = 10^{-3}$ and $n_{\rm i0} = 10^{26}\,{\rm cm}^{-3}$.

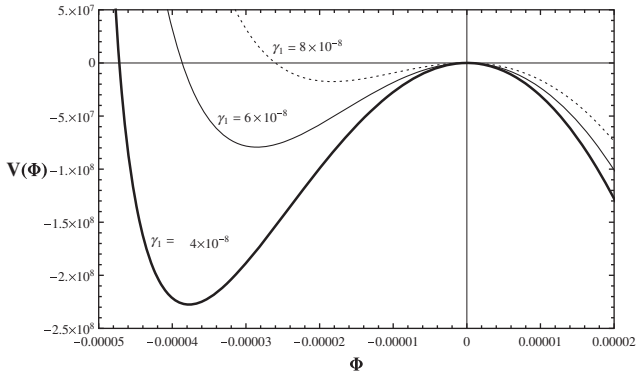

Figure 11. Profile of $V(\Phi)$ for different values of γ_1 when the other parameters are $M = 0.7$, $Z_d = 10^4$, $T_i = 0.1$ and $n_{i0} = 10^{26}$ cm^{-3}.

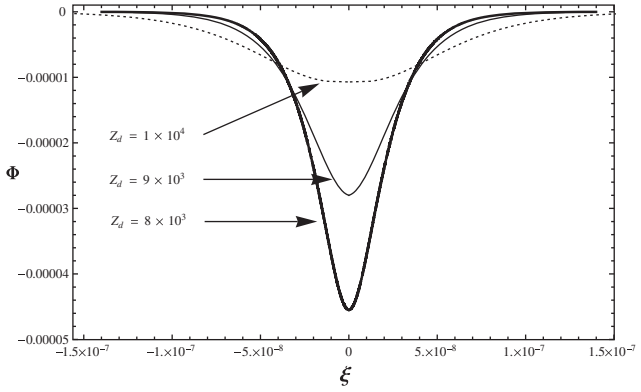

Figure 12. Soliton structures for different values of dust charge number Z_d corresponding to $V(\Phi)$in figure 9.

5. Modulational stability analysis with the Jean term

As noted earlier, when the gravitational Sagdeev potential given by equation (16) is taken into account, the formation of solitary structures is not possible. However, as it is obvious that equations (15) and (16) are coupled, the gravitational potential significantly contributes to the amplitude modulation. In this section, we shall address the question of modulational stability/instability (MI) of the wave and investigate the dependence of MI on the gravitational potential and other parameters of the system. We expand equations (11) and (12), assuming the potentials Φ and Ψ to be small, and restricting the terms up to the square order, we obtain

$$\frac{\mathrm{d}^2\Phi}{\mathrm{d}\xi^2} \approx \frac{2}{3\gamma_2}\left[Z_d\gamma_1\left\{1-\frac{3\gamma_2}{2\gamma_1 Z_d^2 M^2}(Z_d\Phi-\Psi)+\frac{27\gamma_2^2}{8\gamma_1^2 Z_d^4 M^4}\left(Z_d^2\Phi^2-2Z_d\Phi\Psi+\Psi^2\right)\right\}+\gamma_2\left(1+\frac{3}{2}\Phi+\frac{3}{8}\Phi^2\right)-\left(1-\frac{1}{T_i}\Phi+\frac{1}{2T_i^2}\Phi^2\right)\right], \tag{18}$$

$$\frac{\mathrm{d}^2\Psi}{\mathrm{d}\xi^2} \approx \frac{2\gamma_1 Z_d^2\omega_{jd}^2}{3\gamma_2\omega_{pd}^2}\left[1-\frac{3\gamma_2}{2\gamma_1 Z_d^2 M^2}(Z_d\Phi-\Psi)+\frac{27\gamma_2^2}{8\gamma_1^2 Z_d^4 M^4}\left(Z_d^2\Phi^2-2Z_d\Phi\Psi+\Psi^2\right)\right]. \tag{19}$$

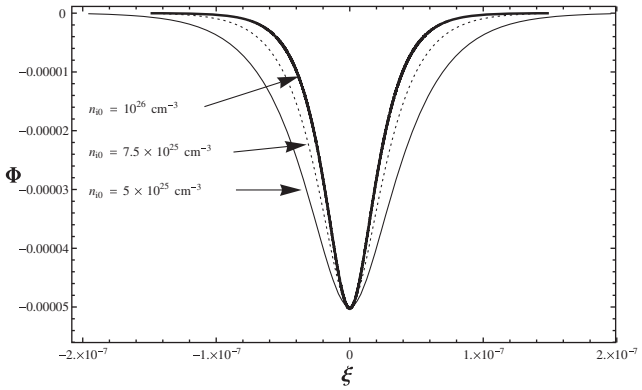

Figure 13. Soliton structures for different values of n_{i0} corresponding to $V(\Phi)$ in figure 10.

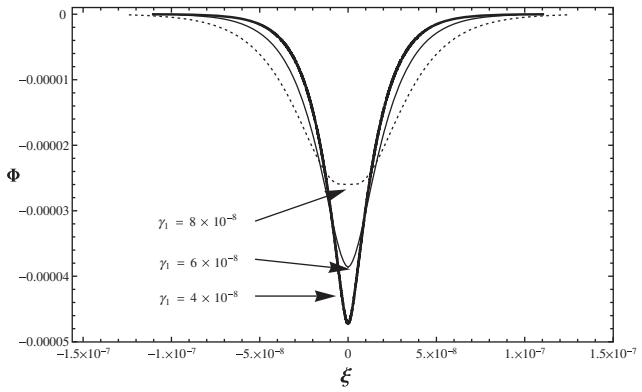

Figure 14. Soliton structures for different values of γ_1 corresponding to $V(\Phi)$ in figure 11.

For modulational stability analysis, we adopt a standard technique in which amplitude is perturbed around some fixed values of Φ_0 and Ψ_0. Thus, by considering $\Phi = \Phi_0 + \delta\Phi$ and $\Psi = \Psi_0 + \delta\Psi$, with $\delta\Phi, \delta\Psi \sim \mathrm{e}^{k_c\xi}$, where k_c is the wave number of modulation when the electrostatic and gravitational potentials are coupled.

The linear stability is checked by supposing solutions of the form $\Phi = \Phi_0 + \alpha_0\exp(\mathrm{k_c}\xi)$ and $\Psi = \Psi_0 + \beta_0\exp(\mathrm{k_c}\xi)$ for the electrostatic and gravitational potentials, respectively. By substituting these solutions into equations (18) and (19), we obtain, to the zeroth order,

$$\Phi_0 = \frac{-\left(b-\frac{9\gamma_2\Psi_0}{4M^2}\right)\pm\sqrt{\left(b-\frac{9\gamma_2\Psi_0}{4M^2}\right)^2-\frac{3a\gamma_2\Psi_0}{Z_d M^2}\left(1+\frac{27\gamma_2\Psi_0}{4\gamma_1^2 Z_d^4 M^2}\right)}}{2a}, \tag{20}$$

$$\Psi_0 = -\left(Z_d\Phi_0+\frac{2\gamma_1 Z_d^2 M^2}{3\gamma_2}\right) \pm\frac{2}{3\sqrt{3}}Z_d M\sqrt{\frac{\gamma_1}{\gamma_2}\left(6Z_d\Phi_0-\frac{5\gamma_1 Z_d^2 M^2}{3\gamma_2}\right)}, \tag{21}$$

where

$$a = \frac{27\gamma_2^2}{4\gamma_1 Z_d^2 M^4}+\frac{3\gamma_2}{4}-\frac{1}{T_i^2}, \tag{22}$$

$$b = \frac{1}{T_i}+\frac{3\gamma_2}{2}-\frac{3\gamma_2}{2M^2}. \tag{23}$$

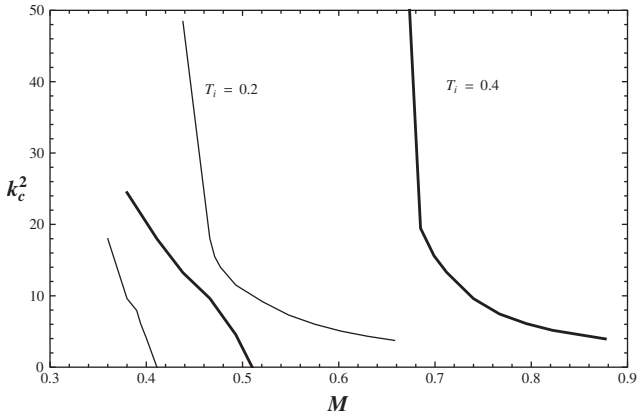

Figure 15. Variation of k_c^2 with M at different values of T_i, the other parameters being $Z_d = 10^3$, $\gamma_1 = 10^{-5}$, $n_{i0} = 10^{24}\,\mathrm{cm}^{-3}$ and $n_{d0} = 10^{19}\,\mathrm{cm}^{-3}$.

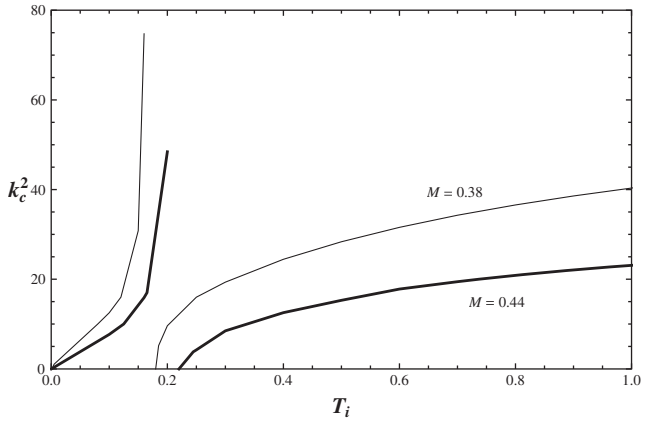

Figure 16. Variation of k_c^2 with T_i at different values of M, the other parameters being $Z_d = 10^3$, $\gamma_1 = 10^{-5}$, $n_{i0} = 10^{24}\,\mathrm{cm}^{-3}$ and $n_{d0} = 10^{19}\,\mathrm{cm}^{-3}$.

Now we collect the first-order terms from equations (18) and (19) and obtain the eigenvalue equation for k_c given by

$$k_c^2 \approx \frac{C}{2}\left[\left(\left(1-\frac{\omega_{pd}^2}{\omega_{jd}^2}\right)AB+D+E\right) \pm\sqrt{\left(\left(1-\frac{\omega_{pd}^2}{\omega_{jd}^2}\right)AB+D+E\right)^2-4AB\,(D+E)}\right], \tag{24}$$

where

$$A=\frac{3\gamma_2\omega_{jd}^2}{2M^2\omega_{pd}^2}, \tag{25}$$

$$B=1-\frac{9\gamma_2}{2\gamma_1 Z_d^2 M^2}\left(Z_d\Phi_0-\Psi_0\right), \tag{26}$$

$$C=\frac{2}{\gamma_1 Z_d^2}, \tag{27}$$

$$D=\frac{1}{T_i}+\frac{3\gamma_2}{2}, \tag{28}$$

$$E=\left(\frac{3\gamma_2}{4}-\frac{1}{T_i^2}\right)\Phi_0. \tag{29}$$

We shall note that plasma is marginally stable if $k_c^2 = 0$, which is satisfied under two independent conditions: either

$$Z_d\Phi_0-\Psi_0=\frac{2\gamma_1 Z_d^2M^2}{9\gamma_2} \quad \text{or } \Phi_0=\frac{(1/T_i)+(3\gamma_2/2)}{(1/T_i^2)-(3\gamma_2/4)}.$$

It is clear from the first condition that the marginal stability is affected not only by the inclusion of gravitational potential but also by the ion temperature and electron to ion concentration shown in the second condition. The wave is unstable if $k_c^2 > 0$, which demands two coupled conditions

$$Z_d\Phi_0-\Psi_0<\frac{2\gamma_1 Z_d^2M^2}{9\gamma_2}, \quad \Phi_0<\frac{(1/T_i)+(3\gamma_2/2)}{(1/T_i^2)-(3\gamma_2/4)} \quad \text{and}$$

$$Z_d\Phi_0-\Psi_0>\frac{2\gamma_1 Z_d^2M^2}{9\gamma_2}, \quad \Phi_0>\frac{(1/T_i)+(3\gamma_2/2)}{(1/T_i^2)-(3\gamma_2/4)}.$$

Here, again the gravitational potential plays a role in setting the Mach number in the instability conditions. Now instability occurs at lower value of Mach number in the presence of gravitational effects of dust particulates.

We have analyzed numerically the variation of k_c^2 with M at different values of ion temperature, i.e. $T_i = 0.2, 0.4$, as shown in figure 15. At $T = 0.2$ the wave faces a narrow cutoff region approximately from $M = 0.41$ to $M = 0.44$ and then with an increase in M the wave changes from being modulationally less unstable. Further, the variation in k_c^2 with T_i at two different values of Mach number, i.e. $M = 0.38$ and 0.44, shown in figure 16 indicates that the wave is modulationally more unstable at lower value of M. The wave is marginally stable ($k_c^2 = 0$) at low ion temperature for comparatively lower values of Mach number. The wave goes from marginal stability to instability, an increase in ion temperature and then faces a narrow cutoff region before again showing marginal stability. The range of the cutoff region changes for different values of Mach number. As is obvious from figures 15 and 16, k_c^2 is always positive; therefore, the wave undergoes a critical instability, not oscillating instability.

6. Conclusions

We have analyzed the DAWs in unmagnetized collisionless self-gravitating plasma by treating the ions to be Maxwellian and considering the electrons to be degenerate and have taken their trapping into account. We employed the Fermi–Dirac distribution for the electrons and expressed electron density in equation (6) that takes into account the effect of temperature. This equation has been used for fully degenerate plasma, namely $T_e = 0$. The nonlinear analysis has been carried out through the Sagdeev potential approach where gravitational effects are neglected. The modification in the soliton profile due to changes in Mach number, density ratio, ion temperature and dust charge number has been investigated numerically, and the results are presented graphically. We also discussed the condition for MI when gravitational effects are taken into account by including the Jean term in our considerations. The effects of the gravitational potential and various other physical parameters on MI have been investigated numerically and the

results are presented graphically. We believe that trapping is a fundamental nonlinear effect that has so far not been investigated in degenerate plasmas with a dust component, and our study presents these results for situations where gravitational effects are not taken into account initially, but then gravitational effects are included to investigate MI.

References

[1] Ali S and Shukla P K 2006 *Phys. Plasmas* **13** 022313
[2] Mushtaq A and Khan S A 2007 *Phys. Plasmas* **14** 052307
[3] Misra A P and Chowdhury A R 2006 *Phys. Plasmas* **13** 072305
[4] Hass F 2007 *Phys. Plasmas* **12** 062117
[5] Salimullah M, Jamil M, Shah H A and Murtaza G 2009 *Phys. Plasmas* **16** 014502
[6] Khan S A, Masood W and Sadiq M 2009 *Phys. Plasmas* **16** 013701
[7] Saeed-ur-Rehman 2010 *Phys. Plasmas* **17** 062303
[8] Markowhich P A, Ringhofer C and Schmeiser C 1990 *Semiconductor Equations* (New York: Springer)
[9] Jung Y F 2001 *Phys. Plasmas* **8** 3842
[10] Opher M, Silva L O, Danger D E and Dawson V K 2001 *Phys. Plasmas* **8** 2454
[11] Chabier G, Douchin F and Potekhin Y 2002 *J. Phys.: Condens. Matter* **14** 9133
[12] Manfredi G and Haas F 2001 *Phys. Rev.* B **64** 075316
[13] Haas F, Garcia L G, Goedert J and Manfredi G 2003 *Phys. Plasmas* **10** 3858
[14] Manfredi G 2005 *Fields Inst. Commun.* **46** 263
[15] Salimullah M, Ayub M, Shah H A and Masood W 2007 *Phys. Scr.* **76** 655
[16] Shokri B and Rukhadze A A 1999 *Phys. Plasmas* **6** 4467
[17] Haas F 2003 *Phys. Plasmas* **12** 062117
[18] Bagchi *et al* 2009 *Int. J. Theor. Phys.* **48** 1132
[19] Misra A P and Bhowmik C 2007 *Phys. Plasmas* **14** 012309
[20] Masood W, Mushtaq A and Khan R 2007 *Phys. Plasmas* **14** 123702
[21] Khan S A and Mushtaq A 2007 *Phys. Plasmas* **14** 083703
[22] Haque Q and Mahmood S 2008 *Phys. Plasmas* **15** 034501
[23] Mahmood S and Mushtaq A 2008 *Phys. Lett.* A **372** 3467
[24] Reach W T, Kuchner M J, Hippel T V, Burrow A, Mullally F, Kilic M and Winget D E 2005 *Astrophys. J.* **635** L161
[25] Narlikar A V and Fu Y Y 2010 *Oxford Handbook of Nanoscience and Technology* vol 3 (New York: Oxford University Press)
[26] Jung Y D 2001 *Phys. Plasmas* **8** 3842
[27] Kremp D, Bornath T, Bonitz M and Schlanges M 1999 *Phys. Rev.* E **60** 4725
[28] Shukla P K and Ali S 2005 *Phys. Plasmas* **12** 114502
[29] Salimullah M, Zeba I, Uzma Ch, Shah H A and Murtaza G 2008 *Phys. Lett.* A **372** 2291
[30] Shukla P K and Stenflo L 2006 *Phys. Lett.* A **355** 378
[31] Ludin J, Marklund M and Brodin G 2008 *Phys. Plasmas* **15** 072116
[32] Masood W, Salimullah M and Shah H A 2008 *Phys. Lett.* A **372** 6757
[33] Ren H, Wu Z, Cao J and Chu P K 2009 *Phys. Plasmas* **16** 103705
[34] Erokhin N S, Zolnikova N N and Mikhailovskaya I A 1995 *Fiz. Plasmy* **22** 137
[35] Sagdeev R Z 1996 *Review of Plasma Physics* vol 4 (New York: Consultant Bureau)
[36] Gurevich A V 1968 *Sov. Phys.—JETP* **26** 575
[37] Siddiqui H, Shah H A and Tsintsadze N L 2008 *J. Fusion Energy* **27** 216
[38] Luque A, Schamel H and Fedele R 2004 *Phys. Lett.* A **324** 185
[39] Shah H A, Qureshi M N S and Tsintsadze N 2010 *Phys. Plasmas* **17** 032312
[40] Misra A P and Chowdhury A R 2006 *Eur. Phys. J.* D **37** 105
[41] Duha S S and Mamun A A 2009 *Phys. Lett.* A **373** 287
[42] Tsintsadze N L and Tsintsadze L N 2008 *Europhys. Lett.* **83** 15005
[43] Michael K-H K 2003 *Adv. App. Math.* **31** 132
[44] Landau L D and Lifshitz E M 1980 *Statistical Physics* part 1 (Oxford: Butterworth-Heinemann)
[45] El-Taibany W F and Wadati M 2007 *Phys. Plasmas* **14** 042302
[46] Xue Qi, Wen-Shan D, Jian-Min C and Shan-Jin W 2011 *Chin. Phys.* B **20** 025203
[47] Farihi J, Zuckerman B and Becklin E E 2008 *Astrophys. J.* **674** 431
[48] Witt E and Lotko W 1983 *Phys. Fluids* **26** 2176